Available online at www.sciencedirect.com
SCIENCE DIRECT®

Journal of the European Ceramic Society 23 (2003) 189–193

www.elsevier.com/locate/jeurceramsoc

Preparation and magnetic properties of titanium-substituted LiZn ferrites via a sol-gel auto-combustion process

Zhenxing Yue*, Ji Zhou, Xiaohui Wang, Zhilun Gui, Longtu Li

State Key Laboratory of New Ceramics and Fine Processing, Department of Materials Science and Engineering, Tsinghua University, Beijing 100084, PR China

Received 26 October 2001; received in revised form 22 February 2002; accepted 3 March 2002

Abstract

A series of nitrate–citrate gels were prepared from metal nitrates and citric acid via a sol-gel process, in order to synthesize titanium-substituted lithium zinc (LiZn) ferrites with composition of $Li_{0.5(0.4+x)}Zn_{0.6}Ti_xFe_{(2.2-1.5x)}O_4$ (x ranging from 0.05 to 0.20). The thermal decomposition process was investigated by DTA-TGA, IR and XRD techniques. The dried gels can burn in a self-propagating combustion process in air to transform into single-phase, nano-crystalline ferrite particles. The low-temperature sintering was realized using the synthesized powders, and the sintered ferrites have fine-grained microstructures and excellent magnetic properties. Appropriate amounts of titanium substituted for Fe in LiZn ferrites can significantly increase the permeability value. The prepared LiZn ferrites are good materials for multilayer chip inductors.

Keywords: Ferrites; LiZn ferrites; Magnetic properties; Sol-gel processes; (Li, Zn) $(Fe, Ti)_2O_4$

1. Introduction

Lithium and substituted lithium ferrites have been found to be very good materials in microwave devices due to their low costs, high resistivity and low eddy current loss.[1] In the preparation of lithium-based ferrites, low-temperature sintering is needed to suppress lithium volatility and oxygen loss during firing. On the other hand, Li ferrites have been also promising substitutes for NiCuZn ferrites in advanced planar ferrite devices, such as multilayer chip inductors (MLCIs), because of their low sintering temperature, high Curie temperature and excellent electromagnetic properties at high frequency.[2] These chip inductors are fabricated by laminating ferrite layers and internal conductors alternatively and then co-firing to form the monolithic structure. Silver, Ag, is usually used as the internal electrode material of MLCIs due to its low resistivity and lower cost. Therefore, low-temperature sintered ferrites are required for MLCIs. Usually, liquid-phase agents such as Bi_2O_3 and SiO_2-bassed glasses have been used to promote the low-temperature densification.[2–4] However, the additives, which form glassy phases at grain-boundaries in sintered ferrite, generally deteriorate the electromagnetic properties of MLCIs.[5] Therefore, low-temperature sintered ferrites without low-melting additives are especially required to meet the requirement of high performance MLCIs.

It is well known that low-temperature sintering of ferrites can be achieved by using active ultrafine powders synthesized via a wet-chemical method. Several chemical processing techniques, such as hydrothermal, sol–gel, co-precipitation and combustion synthesis have been investigated to prepare ultrafine ferrite powders.[5–10] Among these techniques, combustion synthesis has been proved to be a simple and economic way to prepare nanoscale powders.[11–13] In this technique, a thermally induced anionic redox reaction takes place. The energy from the exothermic reaction between oxidant and reductant can be high enough to form a desirable phase within a very short time. In our previous works,[14,15] we synthesized nanocrystalline NiCuZn ferrites using auto-combustion of nitrate–citrate gel, in which nitrates provided metal ions and citric acid acted as gelatin agent. The synthesized ferrites have high sintering activity and excellent electromagnetic properties.

* Corresponding author. Tel.: +86–10-62784579; fax: 86–10-62771160.

E-mail address: yuezhx@tsinghua.edu.cn (Z. Yue).

0955-2219/02/$ - see front matter
PII: S0955-2219(02)00082-1

In the present work, we focus on the synthesis of titanium-substituted LiZn ferrite powders by the sol-gel auto-combustion technique. In this paper, we report on the synthesis process, characterization, and the magnetic properties of as-sintered ferrites from the nano-sized powders.

2. Experimental procedure

The titanium-substituted LiZn ferrites with composition of $Li_{0.5(0.4+x)}Zn_{0.6}Ti_xFe_{(2.2-1.5x)}O_4$ (x ranging from 0.05 to 0.20) were prepared by sol-gel auto-combustion. All chemicals used were of reagent grade purity. $LiNO_3$, $Zn(NO_3)_26H_2O$, and $Fe(NO_3)_39H_2O$ were used to incorporate metal ions needed. Butyl titanate, $(C_4H_9O)_4Ti$, was used as a source of Ti^{4+} ions.

The ferrite powders were synthesized as follows. Appropriate amounts of metal nitrates, $(C_4H_9O)_4Ti$ and citric acid, which could form 50 g of titanium-substituted LiZn ferrite powder, were first dissolved in 600 ml of deionized water. The molar ratio of nitrates to citric acid was 1:1. A small amount of ammonia was added to the solution to adjust the PH value to about 7. During this process, the solution was continuously stirred using a magnetic agitator. Then, the mixed solution was poured into a dish and heated at 120 °C stirring constantly to transform into a xerogel. When ignited at any point, the dried gel burned in a self-propagating combustion manner until all gels were burned completely out to form loose powders.

The synthesized ferrite powders were mixed with an appropriate amount of 5wt% poly(vinyl alcohol) as a binder, and granulated using a 60-mesh sieve. The granulated powders were uniaxially pressed at a pressure of 100 MPa to form green toroidal specimens. The specimens were heated at a rate of 5 °C/min to 950 °C, and soaked for 8 h in air, then cooled at a rate of 4 °C/min to room temperature.

The dried gels were characterized via thermogravimetric (TGA) and differential thermal analysis (DTA) (SETARAM 92) at a heating rate of 10 °C/min in static air. The phase identification of the gel precursors and as-burnt powders was performed using Rigaku D/MAX IIIB X-ray diffractometer (XRD) with CuK_α radiation. Infrared spectra (IR) for the gel precursors and as-burnt powders were recorded on a PE883 spectrophotometer from 500 to 4000 cm^{-1} by the KBr pellet method. The average crystallite sizes of the synthesized powders were determined by using the XRD patterns, via the well-known Scherrer equation. The microstructure of sintered ferrites was observed by scanning electron microscope (SEM, Hitachi S450). Initial permeability (μ_i) and quality factor (Q) of sintered toroidal specimens were measured using a HP4194 impedance analyzer.

3. Results and discussion

3.1. IR spectra of gel precursors and as-burnt powders

It was observed in our experiment that the dried gels, formed from metal nitrates and citric acid with the molar ratio of 1:1, exhibit self-propagating combustion behavior, as observed in our previous work.[13] When the dried gel was ignited at any point in the air, the combustion rapidly propagated forward until all the gels were completely burnt out to form loose powders.

IR spectra of the dried gels and as-burnt powders were examined to investigate the chemical and structural changes that take place during this combustion process. Fig. 1 shows the typical IR spectra of the dried gels and as-burnt powders in the range 500–4000 cm^{-1}. It is clearly seen from the figure that the dried gels show several absorption bands at about 3160, 1650, and 1380 cm^{-1} corresponding to the O–H group, carboxyl group and NO_3^- ions respectively. The appearance of the characteristic bands of NO_3^- indicates that the NO_3^- exists as a group in the structure of citrate gel during the gelation of mixed solution formed from nitrates and citric acid. In the IR plots of powders after combustion, the absorption band at $\sim$1380 cm^{-1}, which corresponds to NO_3^- ions, disappears. And the bands at $\sim$1650 cm^{-1} and 3160–3450 cm^{-1} reduce significantly. On the other hand, a significant spectroscopic band at $\sim$560 cm^{-1} appears. This band is identified to be the characteristic absorption band of ferrite. Thus, the decrease or disappearance of the characteristic bands of carboxyl groups and NO_3^- ions in the IR spectrum curve after combustion suggests that carboxyl groups and NO_3^- ions take part in the reaction during combustion.

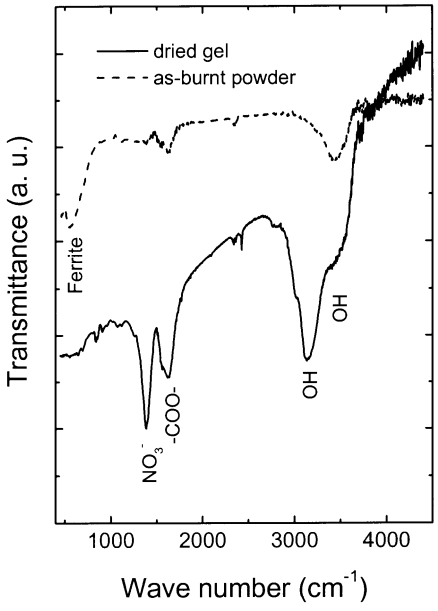

Fig. 1. Typical IR spectra of the dried gels and as-burnt powders.

Therefore, the combustion can be considered as a thermally induced anionic redox reaction of the gel wherein the carboxyl groups act as reductant and NO_3^- ions act as oxidant, as reported by Chakrabarti [11] and Schafer [12]. The energy from the reaction between oxidant and reductant may be high enough to form ferrite phase within a very short time. Because the NO_3^- ions in gel provide an in situ oxidizing environment for the decomposition of the organic component, as well as the heat released from the exothermic reaction, the rate of oxidation reaction relatively increases, resulting in a self-propagating combustion process.

3.2. DTA characterization of dried gels

The autocatalytic combustion process of the nitrate–citrate gels was investigated by thermal analysis (DTA and TG) of the dried gels. Fig. 2 shows the DTA and TG plots of the dried gel with titanium concentration of 0.05. As expected, the decomposition reaction is strongly exothermic. The exothermic peak, at ~210 °C, is relatively sharp and intense. This indicates that the decomposition of the gel occurs suddenly in a single step, as observed in other systems.[12–14] It has been concluded that the exothermic peak in the DTA plot of nitrate-citrate gel corresponds to an autocatalytic anionic oxidation–reduction reaction between the nitrate and citrate system.

Moreover, it was observed that the combustion process depends on the concentration of titanium. Fig. 3 shows the DTA plots for the dried gel with titanium content of 0.05 and 0.15. Comparing the two plots, we can see that the exothermic peak at ~210 °C reduces, while the subsequent exothermic peak at ~430 °C increases for 0.15 titanium gel. It is believed that the main exothermic peak corresponds to the redox reaction between nitrate ions and carboxylate anions. The subsequent peak is believed to be due to combustion reaction of excess carboxylate anions. Therefore, we can conclude that the observed decrease of combustion rate with increase of titanium content may be attributed to the increase of carboxylate due to the incorporation of titanium from $(C_4H_9O)_4Ti$.

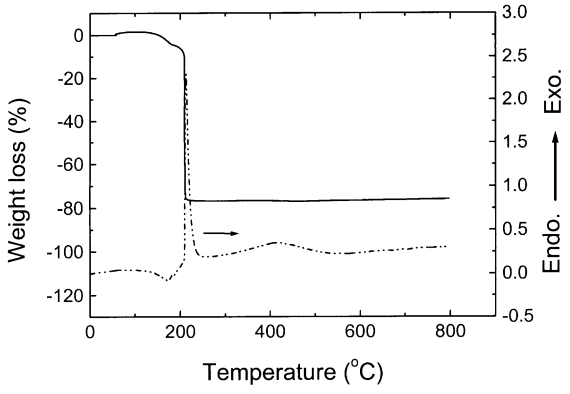

Fig. 2. DTA and TGA plots of the dried gel with titanium concentration of 0.05.

3.3. Phase analysis and particle sizes of powders

Powder X-ray diffraction studies (XRD) have been carried out on the dried gels, as-burnt powders, and ceramic samples sintered at 950 °C, respectively. Fig. 4 shows the XRD patterns for the dried gels and the as-burnt powders with different contents of titanium. It is clear that the dried gels are amorphous in nature. All the as-burnt powders are single-phase ferrites with spinel structure. This indicates that the titanium-substituted LiZn ferrite can be directly formed after auto-combustion of gel, not required calcination at high temperature as in other synthesis techniques.

The average crystallite sizes of the synthesized powders were determined by using the X-ray peak broadening of the (311) diffraction peak, via the well-known Scherrer equation. Fig. 5 shows the average crystallite

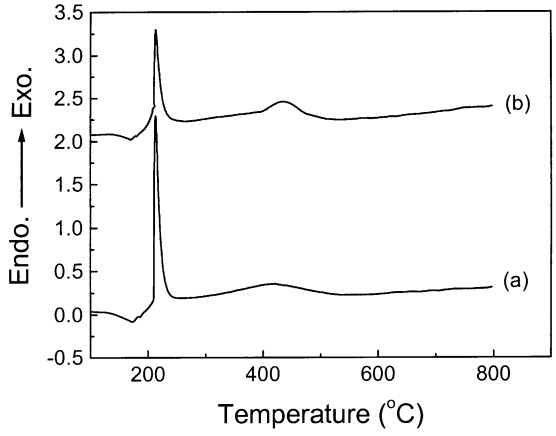

Fig. 3. DTA plots for the dried gel with titanium content of 0.05 (a) and 0.15 (b).

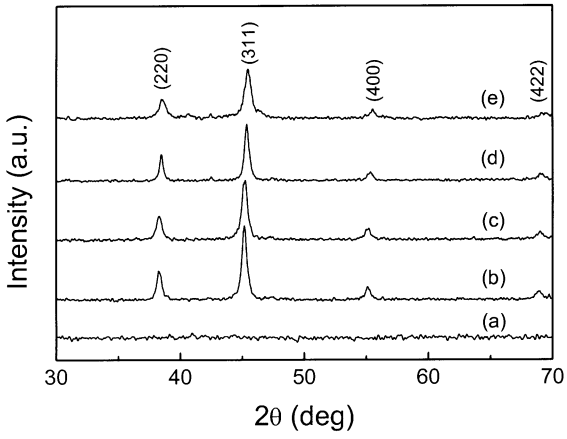

Fig. 4. XRD patterns for the dried gel and the as-burnt powders with different contents of titanium, (a) dried gel, (b) $x=0.05$, (c) $x=0.10$, (c) $x=0.15$, (d) $x=0.20$, and (e) $x=0.20$.

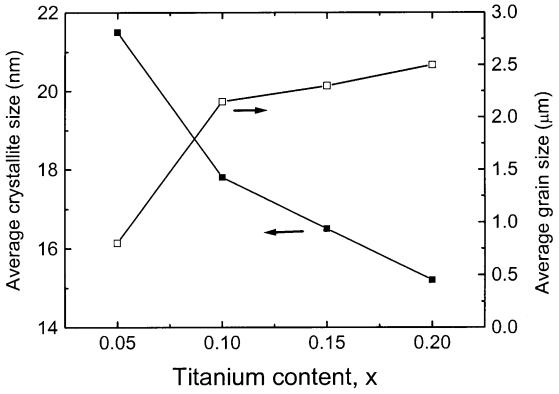

Fig. 5. Average crystallite size of the synthesized powders and grain size of the sintered ferrites as a function of titanium concentration.

size of the synthesized powders as a function of the content of titanium. It is clearly seen from the figure that the synthesized powders are nanocrystalline particles with crystallite size of 15–22 nm. The decreased combustion rate and heat released from reaction may be responsible for the decrease of the crystallite size with the increase of titanium.

3.4. Microstructure and magnetic properties of sintered LiZn ferrites

The synthesized ferrite powders were granulated using PVA as a binder, and uniaxially pressed to form green toroidal specimens. Then, the specimens were sintered in static air. It was observed that the well-densified bodies were obtained after sintering at 950 °C for 8 h, showing the high sintering activity of nano-sized ferrite powders. The XRD patterns of the sintered ferrites revealed single-phase spinel structure for all samples. No effect of titanium on the crystalline phase was observed. The density, grain size and main magnetic properties of the sintered ferrites are shown in Table 1.

The microstructure of sintered ferrites was observed by scanning electron microscope (SEM). The well-densified and uniform microstructures are observed from the photographs, and the average grain size was taken by line-section method. The values of average grain size were given in Table 1 and were plotted as a function of titanium content in Fig. 5. It can be observed that the grain size increases with increasing the content of titanium. The average grain sizes for all samples are about 1–2.5 μm, exhibiting fine-grained microstructure with respect to that of the ferrites prepared by the conventional route. This is preferable to the high performance MLCIs with thinner internal ferrite layers.

The frequency dependence of the initial permeability for titanium-substituted LiZn ferrites is shown in Fig. 6. Flat permeability profiles are observed at frequencies up to 1 MHz for all samples, exhibiting good frequency stability. The composition dependencies of permeability and quality factor are also observed from the figure and Table 1. The maximum permeability value of more than 600 is obtained at the titanium concentration of 0.15. This suggests that appropriate amounts of titanium substituted for Fe in LiZn ferrites significantly increase the permeability. The magnetization change caused by the substitution of non-magnetic ions in ferrite structure may be responsible for the changing of permeability as a function of titanium concentration.

It is well known that LiZn ferrite is an inverse spinel with lithium ions occupying the octahedral sites and zinc ions occupying the tetrahedral sites. In titanium-substituted LiZn ferrite, the Fe^{3+} ions in the B site are replaced by lithium and titanium ions. As observed from Fig. 6, the permeability value shows a maximum at the concentration of titanium of 0.15 and a decrease on further addition of titanium. A similar behavior was also observed in LiTiZn ferrites prepared via the conventional method by Manjula et al.[16] They reported that the net magnetization and Curie temperature values of titanium substituted LiZn ferrites increase with the concentration of titanium and reach a maximum at the titanium concentration of 0.56. A further increase in the concentration of non-magnetic ions weakens the inter-site exchange interaction, and values of Curie temperature and magnetization decrease. This was attributed to canting of spins at higher concentration of non-magnetic substitution.[17] Compared to those of Manjula,[16] the decrease in the concentration of titanium, at which the maximum permeability occurs, may be caused from the uniform distribution of ions in ferrites prepared via the sol-gel route. The other factor, which is responsible for the increase in permeability

Table 1
Density, grain size and main magnetic properties of sintered Ti-substituted LiZn ferrites

Ti concentration	Density (g/cm^3)	Grain size (μm)	Initial permeability (100 kHz)	Quality factor (100 kHz)	Curie temperature (°C)	α_μ[a] ($\times 10^{-6}$/°C)
0.05	4.64	0.8	273	32.0	>200	9.7
0.10	4.63	2.2	590	28.7	172	6.3
0.15	4.66	2.3	613	27.4	152	5.6
0.20	4.61	2.5	413	36.0	143	5.3

[a] α_μ, The temperature coefficient of permeability in the range of temperature from −25 to +85 °C.

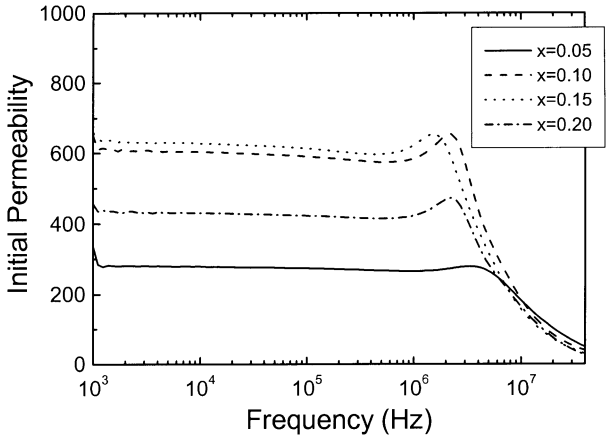

Fig. 6. Frequency dependence of the initial permeability for $Li_{0.5(0.4+x)}Zn_{0.6}Ti_xFe_{(2.2-1.5x)}O_4$ ferrites.

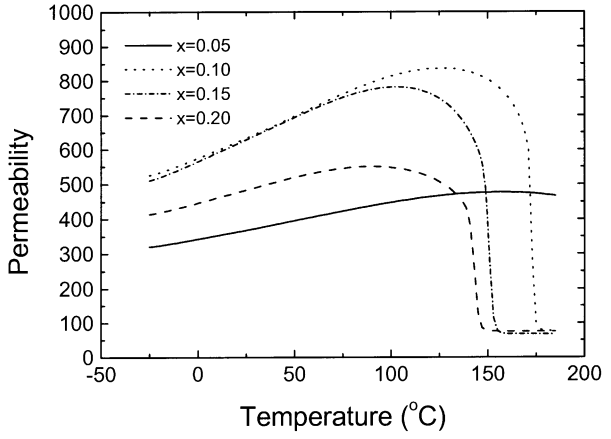

Fig. 7. Temperature dependence of permeability for $Li_{0.5(0.4+x)}Zn_{0.6}Ti_xFe_{(2.2-1.5x)}O_4$ ferrites.

value from the titanium concentration of 0.05–0.10, may be the increase in grain size.

Fig. 7 shows the temperature dependence of permeability for titanium-substituted LiZn ferrite. It is clearly seen from the figure and Table 1 that the Curie temperature decreases with increasing the concentration of titanium ions from 0.05 to 0.20. This may be originated from the non-magnetic nature of titanium ions, which may break linkages between magnetic cations. No maximum value of Curie temperature occurs in the compositions studied. This is consistent with the observation of Baba et al. in LiTiZn ferrites,[18] but not consistent with Manjula's observation.[16]

Although the Curie temperature reduces with incorporation of titanium, the temperature stability of permeability in the range of temperature from −25 to +85 °C is good for all samples. The temperature coefficient of permeability, shown in Table 1, is less than $1\times10^{-5}/°C$, meeting the requirement of MLCIs.

4. Summary

A series of nitrate–citrate gels were prepared from metal nitrates and citric acid by sol-gel process, in order to synthesize titanium-substituted lithium zinc (LiZn) ferrites with composition of $Li_{0.5(0.4+x)}Zn_{0.6}Ti_xFe_{(2.2-1.5x)}O_4$ (x ranging from 0.05 to 0.20). The nitrate–citrate gels can burn in a self-propagating combustion way. After combustion, the gels directly transform into single-phase, nano-crystalline titanium-substituted LiZn ferrite particles. The average crystallite size of the synthesized powders decreases with increasing titanium concentration. The ferrites sintered at 950 °C possess fine-grained microstructures and excellent magnetic properties. Appropriate amounts of titanium substituted for Fe in LiZn ferrites can significantly increase the permeability. The maximum permeability value of more than 600 is obtained at the titanium concentration of 0.15. The prepared titanium-substituted LiZn ferrites can be used for multilayer chip inductors.

Acknowledgements

This work has been financially supported by the National Natural Science Foundation of China (Grant No. 59995523) and the High Technology Research and Development Project of China.

References

1. Pardavi-Horvath, M., *J. Magn. Magn. Mater.*, 2000, **171**, 215–216.
2. Zhou, J., Liang, B., Zhang, H., Yue, Z., Gui, Z. and Li, L., *High Tech. Lett.*, 1998, **8**(4), 39.
3. Paria, M., Maiti, C. K. and Chakrabarti, N. B., *J. Mater. Sci.*, 1982, **17**, 1459.
4. Brooks K. G., Berta Y. and Amarakoon, V. R. W., *J. Am. Ceram. Soc.*, 1992, **75**(11),3065
5. Fujimoto, M., *J. Am. Ceram. Soc.*, 1994, **77**(11), 2873.
6. Dias, A. and Buono, V. T. L., *J. Mater. Res.*, 1997, **12**(12), 3278.
7. Pavindranathan, P. and Paril, K. C., *Am. Ceram. Soc. Bull.*, 1987, **66**(4), 688.
8. Kumar, P. S. A., Shrotri, J. J. and Kulkarni, S. D., *Mater. Lett.*, 1996, **27**, 293.
9. Suresh, K. and Patil, K. C., *J. Solid State Chem.*, 1992, **99**, 12.
10. Cho, Y. S., Burdick, V. L. and Amarakoon, V. R. W., *J. Am. Ceram. Soc.*, 1999, **82**(6), 1416.
11. Chakrabarti, N. and Maiti, H. L., *Mater. Lett.*, 1997, **30**, 169.
12. Schafer, J., Sigmand, W., Roy, S. and Aldinger, F., *J. Mater. Res.*, 1997, **12**(10), 2518.
13. Yue, Z., Li, L., Zhou, Ji., Zhang, H. and Gui, Z, *Mater. Sci. Eng.*, 1999, **B64**, 68.
14. Yue, Z., Zhou, J., Li, L., Zhang, H. and Gui, Z., *J. Magn. Magn. Mater.*, 2000, **208**, 55.
15. Yue, Z., Zhou, J., Li, L. and Gui, Z., *J. Magn. Magn. Mater.*, 2001, **233**, 224.
16. Manjula, R. and Sobhanadri, J., *J. Magn. Magn. Mater.*, 1988, **75**, 371.
17. Patton, C. E., *J. Appl. Phys.*, 1982, **53**, 2431.
18. Baba, P. D., Argentina, G. M., Courtney, W. E., Dionne, G. F. and Temme, D. H.. *IEEE Trans. Magn. MAG-8, 1972, 83.*